Phys. Status Solidi C **8**, No. 6, 1888–1892 (2011) / **DOI** 10.1002/pssc.201000155

physica status solidi c
www.pss-c.com
current topics in solid state physics

Matrix metalloproteinase sensing via porous silicon microcavity devices functionalized with human antibodies

Marta Martin[*,1], Chakib Taleb Bendiab[2], Laurent Massif[2], Gabriela Palestino[3], Vivechana Agarwal[4], Frédéric Cuisinier[2], and Csilla Gergely[1]

[1] GES-UMR 5650, CNRS, Université Montpellier 2, Pl. Eugéne Bataillon 34095, Montpellier Cedex 5, France
[2] EA4203, Faculté d'Odontologie, Université Montpellier 1, Montpellier Cedex 5, France
[3] Facultad de Ciencias Químicas, Universidad Autónoma de San Luis Potosí, Av. Salvador Nava 6, 78000 San Luis Potosí, Mexico
[4] CIICAP, Universidad Autónoma del Estado de Morelos, Av. Universidad 1001, Col Chamilpa, Cuernavaca, Mor., Mexico

Received 28 April 2010, revised 7 July 2010, accepted 8 July 2010
Published online 25 November 2010

Keywords porous silicon microcavities, matrix metalloproteinase, AFM, SEM, FT-IR spectroscopy

* Corresponding author: e-mail marta.martin@ges.univ-montp2.fr, Phone: (00) 33 461473248, Fax: (00) 33 461473760

Porous silicon microcavity (PSiMc) structures were used as support material for specific sensing of matrix metalloproteinases (MMPs). For lower concentrations of MMP-8, the structures were tested with two types of functionalization methods. Silanization of the oxidized porous silicon structures, followed by glutaraldehyde chemistry was found to give very inconsistent results. The use of biotinilated bovin serum albumin linked to the naked PSiMc was found to be an alternative method to attach the anti MMP-8 human antibody, previously modified with streptavidin, which was further used to sense MMP-8.

1 Introduction The ability to immobilize biological molecules within porous scaffolds may lead to the development of easy-to-use, sensitive, robust and inexpensive biosensor for the detection of biological substances. In this work, we are interested in detection of matrix metalloproteinases, the major enzymes that degrade extracellular matrix proteins and play a key role in diverse physiological and pathological processes, including embryonic development, wound repair, inflammatory diseases and cancer [1, 2]. They constitute a multigene family of approximately 25 secreted soluble and membrane-tethered enzymes that cleave a variety of substrates. The MMPs are structurally related zinc-dependent endopeptidases and they can be classified according to their primary structure and substrate specificity. According to their structural and functional properties, the MMP family can be subdivided into five groups: (i) the collagenases (MMPs-1, 8 and 13), (ii) the gelatinases A and B (MMPs-2 and 9), (iii) the stromelysins 1 and 2 (MMPs- 3 and 10), (iv) a more heterogeneous subgroup containing matrilysin (MMP-7), enamelysin (MMP-20), the macrophage metalloelastase MMP-12 and MMP-19 and (v) the membrane-type MMPs (MT-MMPs-1 to -4 and stromelysin-3, MMP-11). These MMPs share a common multidomain structure, but are glycosylated to different extents and at different sites. According to sequence alignments [3-5], the assembly of these domains might have been an early evolutionary event, followed by diversification [6]. All MMPs are synthesized with a 20-amino acid residue signal peptide and are (except probably the MT-MMP-like furin-processed proteinases) secreted as latent pro-forms.

In this work, we are interested in detecting the collagenase-type MMP-8 that is an inflammatory marker in gingival fluid for predicting tooth movement during orthodontic treatment [7]. As presence of MMP-8 in saliva is directly related with the tooth movement during orthodontic treatment, monitoring the MMP-8 variation is primordial. Moreover, the amount of MMP-8 in the gingival fluid is gradually growing from a physiological threshold when orthodontic movement, gingivitis and finally periodontitis occur. Current methodology used to quantify the MMPs is

based on ELISA immune assay that needs a large sampling volume and high concentration to quantify the enzyme.

An alternative approach is to use PSiMc, a versatile nano/micro porous structure with a number of unique optical properties that can be used for biosensing applications. The use of porous scaffolds to immobilize biological molecules opens new avenues to further fabrication of biological sensors with high specificity and sensitivity [8]. Porous silicon microcavity (PSiMc) is a good candidate for such applications due to its high surface area (200 m^2/cm^3) [9] and its tuneable average pore size (the pore size changes depending on the electrochemical preparation conditions). PSiMc is a 1-D photonic structure composed of a luminescent single layer or active layer placed between two Bragg reflectors. The remarkable optical properties of PSi structures have already been used for enzyme detection [10] and to engineer light emitting PSi devices [11]. PSiMc may be also used to enhance the sensitivity to detect molecules and biomolecules trapped in the porous structure. For this purpose, the sensing principle in PSi structures is based in the effective refractive index of PSi multilayer that is defined by the porosity and the refractive index of the medium inside the pores. In particular, the cavity mode in its optical spectrum is very sensitive to a change in the refractive index when a molecule is attached to the internal surface of the PSiMc. Selective incorporation of an organic molecule within the PSiMc can modify the refractive index by increasing the average refractive index (n) of the medium in the pores by replacing air (n=1) with organic matter (n>1).

On the other hand, the spectral position of the cavity mode in the photonic band gap can be tuned by varying the electrochemical etching conditions during PSiMc preparation (i.e. by changing the porosity and thickness).

We report on the fabrication of functionalized PSiMc structures for detection of MMPs. Detection of fluorescent molecules using the optical properties of specific PSi structures was recently reported by our team [12, 13]. For this study, we have used FT-IR spectroscopy to investigate and optimize stable functionalized porous silicon microcavities to elaborate a new biosensor for detection of the matrix metalloproteinase MMP-8. The pore dimensions of the used PSiMc structures were evaluated by scanning electron microscopy (SEM) and atomic force microscopy (AFM).

2 Experimental PSiMc structures were prepared as multilayered stacks of low and high refractive indices of 1.13 and 1.4 respectively (calculated at 1500nm by interferometeric method) and with layer thicknesses in the range of visible light wavelength by wet electrochemical etching of highly boron-doped silicon wafer (p++ type, boron-doped, 0.001-0.002 $\Omega \cdot cm^{-1}$, <100> oriented). The first layer of the structure was etched at 80 mA/cm^2 to create macropores with diameters up to 200 nm, assuring good penetration of molecules. For the second layer the current density was reduced to 40 mA/cm^2. An anodization time of 6.4 s (for high current density) and 11.5 s (for low current density) was used for the fabrication of 10 period dielectric Bragg mirrors. To stabilize the PSi multilayer structure, all the samples were thermally oxidized at 900 °C for 10 min. Pore dimensions were evaluated by SEM and AFM in order to determine the surface morphology of PSiMc.

Then, PSiMc scaffolds were modified using two functionalization methods. The first one consisted of PSiMc silanization (APTES) and amine-activation by glutaraldehyde (GLU). The silanization of PSiMc was performed at room temperature by placing the surfaces in 10% v/v 3-(Mercaptopropyl)trimethoxysilane in toluene for 1 h. After silanization, samples were rinsed three times (1 min each) with toluene, ethanol and dried under a stream of N_2. Samples were subsequently functionalized with human antibodies (anti-MMP-8) for MMP-8 detection.

For the second procedure, biotinilated bovin serum albumin was linked to the bare PSiMc and used as an alternative method to attach the anti MMP-8 human antibody, previously modified with streptavidin, which was further used to sense MMP-8. The effect of applied human antibody concentration has been studied for optimal MMP-8 binding. Functionalization with biotinilated bovin serum albumin (BBSA, from Sigma) was carried out at room temperature by placing the surfaces in a 100 μM BBSA solution for 1hr, then samples were rinsed with phosphate buffer (pH 7.2), distilled water and dried under a stream of N_2. Prior to infiltration of the antibody, anti-MMP-8 was modified using the Lighting-Link™ streptavidin conjugation kit (Innova Biosciences). For both functionalization methods, anti-MMP-8 and MMP-8 (Abcam) were prepared in phosphate buffer. The oxidized and functionalized PSiMc surfaces were incubated for 1 hr in both the antibody and the enzyme. Finally, the samples were rinsed with buffer, distilled water and dried under a stream of N_2.

For the sample characterization, Scanning electron micrographs were taken using a Field Emission Quante 200 SEM with 15 kV field emission source. AFM images were recorded in air, with an Asylum MFP-3D head and Molecular Force Probe 3D controller (Asylum Research, Santa Barbara, CA, USA). The AFM images were taken using tapping mode at 1 Hz scan rate and digitized in 512x512 pixels. Rectangular silicon nitride cantilevers from Olympus (OMCL-RC800PSA, Tokyo, Japan) were used at a drive frequency of 18 kHz. Reflectance spectra were measured using a Bruker 66V Fourier Transform Infrared Spectrophotometer (100 scans and resolution 4 cm^{-1}) equipped with a specular reflection unit at a 11º fixed angle and detecting the reflected beam by means of a silicon diode detector.

3 Results and discussion

3.1 Surface characterization Scanning electron microscopy images of the used non-oxidized PSiMc scaffolds are shown in Fig. 1. The cross-sectional image depicts a PSiMc composed by two Bragg mirrors with depths of 1.7 μm and an active layer of 370 nm thickness.

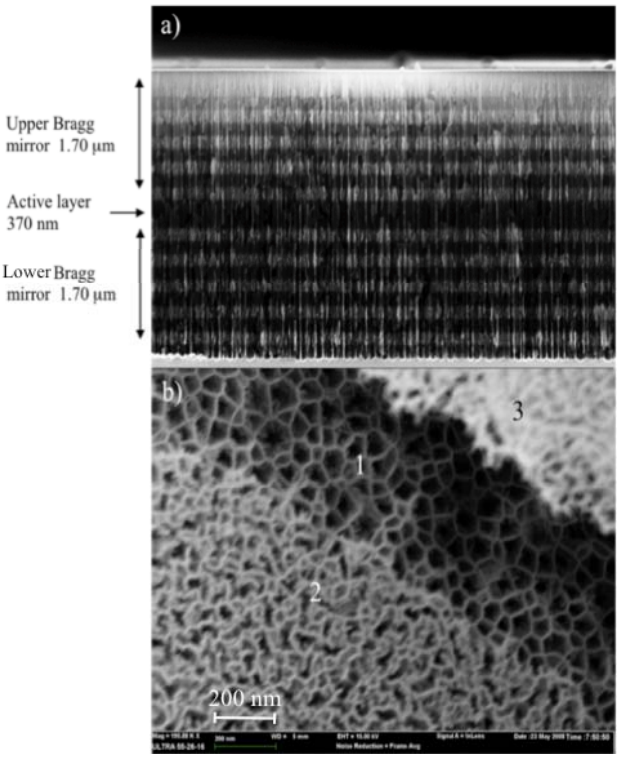

Figure 1 Cross-sectional (a) and top view (b) SEM images of the typical PSiMc used in this work. The cross-sectional image depicts the two Bragg mirrors and the active layer. The top view shows a crack of the topmost part of the first layer (region 2, 3). Through the crack we can observe the actual pore size of the high porosity layer (region 1).

Moreover, the top view shows the high porosity layer (region 1). Average pore size diameters range from 100 to 200 nm. On the other hand, oxidized PSiMc AFM images were acquired to determine the surface morphology such as external pore diameter size and roughness (see Fig. 2). The analysis (from 50 points) shows that PSiMc samples have external pore average diameters of around 100 up to 350nm. Actually oxidation results in opening of the pores, shifting the pore size distribution towards larger diameters [14]. Furthermore, the porous silicon surface roughness quantified in terms of rms (root-mean-square) is 12 nm.

3.2 PSiMc optical detection Specular Reflectometry monitored both functionalization and MMP-8 infiltration into the PSi structure, for a range of MMP-8 concentrations. PSiMc is characterized by a narrow resonance peak in the optical spectrum that is very sensitive to a small change in the refractive index, such as that obtained when a molecule is attached to the large internal surface of porous silicon. Reflectance spectra of the PSiMc were recorded after each modification step. The results obtained for a 10 µg/ml concentration of antibodies and of MMP-8 are shown in Fig. 3. The PSiMc cavity mode spectral position in the photonic gap is located at 801 nm.

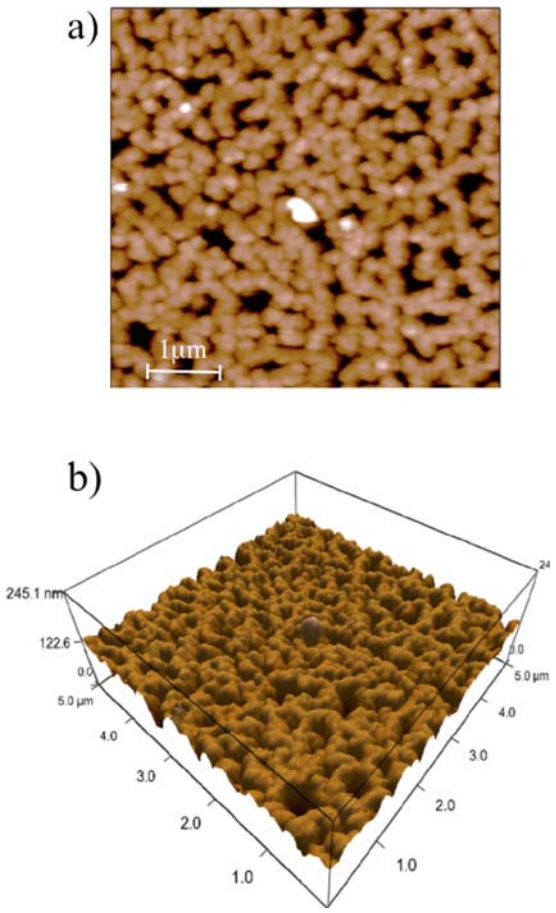

Figure 2 2D (a) and 3D (b) 5X5 µm AFM images of the thermally oxidized PSiMc. The external pore diameters range from 100 to 350 nm.

A first red shift in the reflectance spectra is observed during the surface modification of PSiMc with APTES ($\Delta\lambda_{APTES}$= 11 nm) followed by another red shift after glutaraldehyde activation ($\Delta\lambda_{Glu}$= 6 nm). Furthermore, after anti-MMP-8 and MMP-8 bonding, two strong red shifts ($\Delta\lambda_{Antibody}$= 6 nm, $\Delta\lambda_{MMP\text{-}8}$= 9 nm) were observed. The red shifts recorded are related to the increase in the effective refractive index within the pores due to molecule capture.

We have investigated also other concentrations, down to 100 ng/ml, however our study revealed a great uncertainty in the obtained results for sensing at low concentrations. For such a low concentration, the reproducibility of the results was not satisfactory and most of the time we could not measure any red shift after antibody infiltration. Moreover, several times we even measured a blue shift, as Fig. 4 shows. For this sample, the cavity mode spectral position is located at 776 nm. A first red shift in the reflectance spectra is observed during the surface modification of PSiMc with APTES ($\Delta\lambda_{APTES}$= 26 nm) followed by another red shift after glutaraldehyde activation ($\Delta\lambda_{Glu}$= 13 nm).

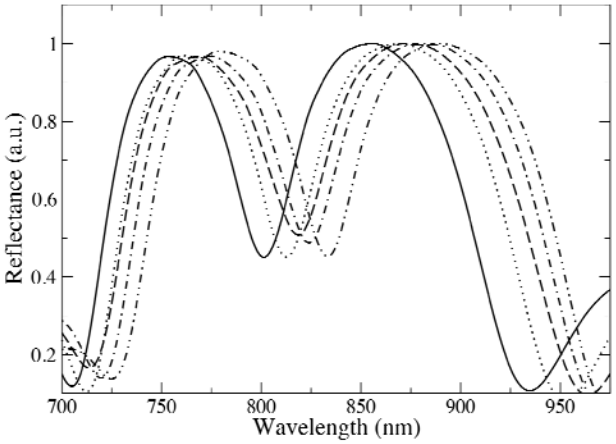

Figure 3 Reflectance spectra of the PSiMc device: (__) as etched, (…) after silanization; (_ _) after glutaraldehyde coupling; (_ . _) after anti-MMP-8 binding and finally (_ .._) after MMP-8 binding, for an antibody and enzyme concentration of 10 μg/ml.

On the contrary, after anti-MMP-8 bonding, one strong blue shift ($\Delta\lambda_{Antibody}$= 6nm) was observed. This indicates not only that anti-MMP-8 is not binding but also that we have removed some of the glutaraldehyde and/or APTES on the surface due to the rinsing procedure performed after each step.

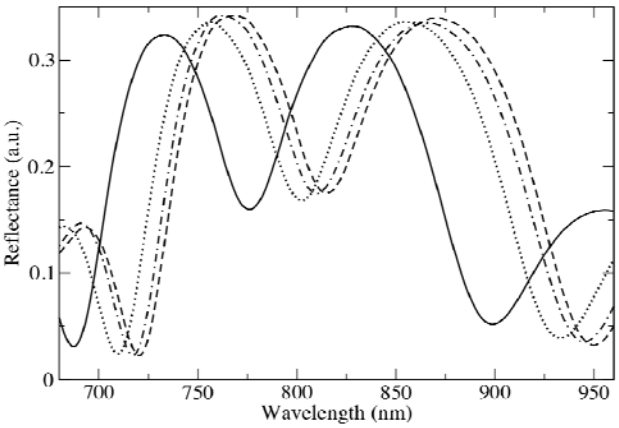

Figure 4 Reflectance spectra of the PSiMc device: (__) as etched, (…) after silanization; (_ _) after glutaraldehyde coupling; and (_ . _) after anti-MMP-8 binding, for an antibody concentration of 100 ng/ml.

We suspect that the applied glutaraldehyde chemistry for antibody binding might cause polymerization leading to inactive molecules that loose their binding capability. This result motivated the use of a second surface functionalization method: attaching biotinilated bovin serum albumin to the naked PSiMc as the only step prior infiltration with anti MMP-8 human antibody at the same low concentration of 100 ng/ml. Figure 5 shows reflectance spectra of the PSiMc recorded after each modification step.

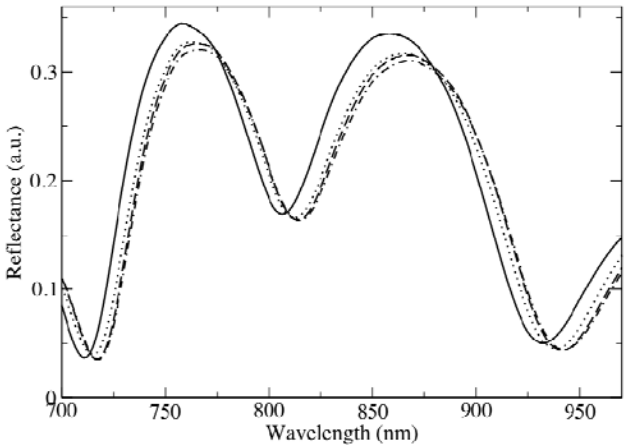

Figure 5 Reflectance spectra of the PSiMc device: (__) as etched, (…) after linking BBSA; (_ _) after anti-MMP-8 binding; and finally (_ . _) after MMP-8 binding for an antibody and enzyme concentration of 100 ng/ml.

The PSiMc cavity mode spectral position is found at 806 nm. A first red shift in the reflectance spectra is observed after BBSA infiltration ($\Delta\lambda_{BBSA}$= 6 nm) followed by subsequent red shifts after anti-MMP-8 ($\Delta\lambda_{Antibody}$= 2 nm) and MMP-8 bonding ($\Delta\lambda_{MMP\text{-}8}$= 2 nm). Hence this functionalization method (via BBSA–streptavidin binding) proved to be much more efficient in detecting very low concentrations (100 ng/ml) of metalloporoteinases, where the currently used silane-glutaraldehyde chemistry failed to work.

4 Conclusions PSiMc is indeed a versatile structure that can be easily used for biosensing applications due to the narrow resonance peak in its optical spectrum that is very sensitive to change in refractive index, when a molecule is attached to its internal surface. Our work demonstrates successful infiltration and detection of the collagenase-type MMP-8 by porous silicon microcavities functionalized with human antibodies. Our results reveal the importance of the applied functionalization procedure when PSiMc structures are used for specific detection via antibodies especially at low concentrations**.** Currently used APTES and glutaraldehyde chemistry might be the cause of polymerization on the surface and on the pore walls of the PSiMc structures leading to antibody/enzyme non-binding. Other functionalization methods, as the use of biotinilated bovin serum albumin in this case, seems to be more adapted for detection of enzymes via antibodies.

Acknowledgements The M06P01 Ecos-North French-Mexican program supported this work. We are grateful to Dr. E. Estephan and M.-B. Saab for fruitful discussions.

References

[1] P. D. Brown and R. Giavazzi, Ann. Oncology **6**, 967 (1995).

[2] H. Nagase and J. F. Woessner, J. Biol. Chem. **274**, 21491 (1999).

[3] R. Beckett and M. Whittaker, Exp. Opin. Ther. Patents **8**, 259 (1998).

[4] K. M. Bottomley, W. H. Johnson, and D. S. J. Walter, Enz. Inhib. **13**, 79 (1998).

[5] I. Massova, L. P. Kotra, R. Fridman, and S. Mobashery, FASEB J. **12**, 1075 (1998).

[6] N. D. Rawlings and A. J. Barrett, Methods Enzymol. **248**, 183 (1995).

[7] S. Apajalahtil, T. Sorsa, S. Railavo, and T. Ingman, J. Dent. Res. **82**, 1018 (2003).

[8] M. Bengtsson, J. Drott, and T. H. Laurell, Phys. Status Solidi A **182**, 533 (2000).

[9] L.A. De Louise and B. L. Miller, Anal. Chem. **76**, 6915 (2004).

[10] M. M. Orozco, C. Pacholsky, G. M. Miskelly, and M. J. Sailor, Adv. Mater. **18**, 1393 (2006).

[11] S. Chan, S. R. Horner, P. M. Fauchet, and B. L. Miller, J. Am. Chem. Soc. **123**, 11797 (2001).

[12] G. Palestino, M.B. dela Mora, J.A. del Río, C. Gergely, and E. Pérez, Appl. Phys. Lett. **91**, 121909 (2007).

[13] M. Martin, G. Palestino, T. Cloitre, V. Agarwal, L. Zimanyi, and C. Gergely, Appl. Phys. Lett. **94**, 223313 (2009).

[14] G. Palestino, R. Legros, V. Agarwal, E. Perez, and C. Ergely, Sens. Actuators B **135**, 27 (2008).

